

Thermodynamic geometry of a black hole surrounded by perfect fluid in Rastall theory

Saheb Soroushfar, ^a Reza Saffari, ^b Sudhaker Upadhyay ^{c,d}

^a*Faculty of Technology and Mining, Yasouj University, Choram 75761-59836, Iran*

^a*Department of Physics, University of Guilan, 41335-1914, Rasht, Iran*

^c*Department of Physics, K.L.S. College, Nawada-805110, India*

^d*Visiting Associate, Inter-University Centre for Astronomy and Astrophysics (IUCAA) Pune, Maharashtra-411007*

E-mail: soroush@yu.ac.ir, rsk@guilan.ac.ir, sudhakerupadhyay@gmail.com

ABSTRACT: In this paper, we study thermodynamics and thermodynamic geometry of a black hole surrounded by the perfect fluid in Rastall theory. In particular, we calculate the physical quantity like mass, temperature and heat capacity of the system for two different cases. From the resulting heat capacity, we emphasize stability of the system. Following Weinhold, Ruppiner, Quevedo and HPEM formalism, thermodynamic geometry of this black hole in Rastall gravity is also analyzed. We find that the singular points of the curvature scalar of Ruppeiner and HPEM metrics entirely coincides with zero points of the heat capacity. But there is another divergence of HPEM metric which coincides with the singular points of heat capacity, so we can extract more information of HPEM metric compared with Ruppeiner metric. However, we are unable to find any physical data about the system from the Weinhold and Quevedo formalism.

Contents

1	Introduction	1
2	Field equations of a black hole surrounded by perfect fluid in Rastall theory	3
3	Black hole surrounded by the quintessence field	4
3.1	Thermodynamics	4
3.2	Thermodynamic geometry	7
4	Black hole surrounded by dust field	9
4.1	Thermodynamics	10
4.2	Thermodynamic geometry	12
5	Concluding remarks	14

1 Introduction

In understanding theory of gravitation, general relativity (GR) follows the covariant conservation of matter energy-momentum tensor. The limitation of such idea is that conservation of energy-momentum tensor has been probed only in the flat or weak-field arena of spacetime. A generalization of this theory, so-called Rastall theory, has recently been proposed, which relaxes the necessity of covariant conservation of the energy-momentum tensor by adding some new terms to the Einstein's equation [1]. Recently, this idea which has been supported in Ref. [2], which shows that the divergence of the energy-momentum tensor can be non-zero in a curved spacetime. Rastall theory provides an explanation for inflation problem and other cosmological problems [3–8]. In order to explain accelerated expansion of universe, one may think that the negative pressure is generated by some peculiar kind of perfect fluid, where the proportion between the pressure and energy density is between 1 and 1/3. If the scalar field generates this perfect fluid, it is generally called quintessence. In Rastall theory of gravitation, the various black hole solutions surrounded by perfect fluid has been discussed [9–14].

Hawking and Bekenstein were first who proposed that black holes have thermodynamic properties [15, 16]. There after, this subject extensively studied by many people [13, 17–24]. In this connection, it has been found that the thermodynamic properties of black holes in Rastall gravity investigate the nature of a non-minimal coupling between geometry and matter fields. Recently, thermodynamics of various black holes under the effect of small thermal fluctuations

have also been studied extensively. For example, thermodynamics of Van der Waals black holes [25], static black hole in $f(R)$ gravity [26], charged rotating AdS black holes [27], black holes in gravities rainbow [28, 29], quasitopological black holes [30], massive gravity black hole [31], Hořava-Lifshitz black hole [32] and Schwarzschild-Beltrami-de Sitter black hole [33] have been discussed.

Meanwhile, several attempts have been made to implement differential geometric concepts in thermodynamics of black holes. In an attempt, to formulate the concept of thermodynamic length, Ruppeiner metric [34], which conformally equivalent to Weinhold's metric [35], is introduced. Furthermore, the phase space and the metric structures suggested that Weinhold's and Ruppeiner's metrics are not invariant under Legendre transformations [36, 37]. Afterwards, another formalism is developed by Quevedo [38], which unifies the geometric properties of the phase space and the space of equilibrium states. Also, a new metric (HPEM metric) [39–41] was introduced in order to build a geometrical phase space by thermodynamical quantities. Though, several study of thermodynamics of various black holes exploiting thermodynamic geometric methods have been made, the thermodynamics of black holes surrounded by perfect fluid in Rastall theory remains unstudied yet. This provides us an opportunity to bridge this gap. This is the motivation of present study.

In this paper, we consider a black hole solution surrounded by the (general) perfect fluid in Rastall theory and describe its thermodynamics by means of two specific cases. In this regard, we first compute mass by setting the metric function representing black hole surrounded by the quintessence field to zero. Furthermore, by exploiting standard thermodynamic relations, we derive the Hawking temperature and heat capacity. The heat capacity plays a pivotal role in describing stability of the black hole. In order to study the behavior of the resulting thermodynamic entities, we plot graphs for them in terms of horizon radius. By doing so, we find that the temperature of black hole surrounded by the quintessence field in Rastall theory remains positive only in a particular range of event horizon for quintessence factor $N_q = 0.05$. The larger values of quintessence factor decrease temperature of the system. This suggests that increasing in the values of quintessence the physical area of this black hole decrease. The heat capacity plot shows that there are physical limitation points and phase transition critical points occurring at different values of event horizons. For this black hole, stability occurs for some particular values horizon radius. We also study the geometric structure of the black hole surrounded by quintessence field by calculating the Weinhold, Ruppiner, Quevedo and HPEM curvature scalars. We find that Weinhold curvature scalar vanishes and becomes fail to describe the phase transition. We obtain a non-zero curvature scalar for the Ruppiner and HPEM geometries and, in these cases, the singular points coincide with zero points of the heat capacity. Also for the HPEM formalism, there is another divergency of HPEM metric which coincides with the singular points of heat capacity and therefore we can extract more information rather than other mentioned metrics. The curvature scalar of Quevedo metric is also calculated. Here, in this case we can't find any physical data about the system.

Moreover, thermodynamic properties of black hole surrounded by dust field in Rastall gravity are also studied. The mass, Hawking temperature and heat capacity of black hole in dust

field background are calculated. In order to do comparative analysis, we plot graphs in terms of horizon radius. From the obtained plots, it is obvious that the mass of the system has one minimum point at particular value of horizon radius. The behavior of temperature with horizon radius is similar to the quintessence case. For instance, increasing the values of dust factor (N_d) the physical area of this black hole decrease. The heat capacity plot tells that stability of black hole increases with the size of black hole upto a certain point. After that point a phase transition occurs and makes the black hole more unstable. We calculate the curvature scalar to discuss the thermodynamic geometry for this case also.

The paper is presented in the following manner. In section 2, we revisit the basic setup of black hole surrounded by perfect fluid in Rastall theory. Thermodynamics and thermodynamic geometry of black hole surrounded by quintessence field are discussed in section 3. Thermodynamics and thermodynamic geometry of black hole surrounded by dust field is presented in section 4. We summarize results and discussions in the last section.

2 Field equations of a black hole surrounded by perfect fluid in Rastall theory

In this section, we briefly review field equations and metric components in the context of Rastall theory. The Rastall field equations for a space-time with Ricci scalar R and an energy momentum source of $T_{\mu\nu}$ can be written as

$$G_{\mu\nu} + k\lambda g_{\mu\nu} = kT_{\mu\nu}, \quad (2.1)$$

where k and λ are the Rastall gravitation coupling constant and the Rastall parameter which indicates deviation scale from the standard GR, respectively. The metric of a black hole surrounded by perfect fluid in Rastall theory would be deduced as follows [12]

$$ds^2 = -f_s(r)dt^2 + \frac{dr^2}{f_s(r)} + r^2(d\theta^2 + \sin^2\theta d\phi^2), \quad (2.2)$$

with

$$f_s(r) = 1 - \frac{2M}{r} + \frac{Q^2}{r^2} - \frac{N_s}{r^{\frac{1+3w_s-6k\lambda(1+w_s)}{1-3k\lambda(1+w_s)}}}. \quad (2.3)$$

where subscript ‘‘s’’ represents the surrounding field, N_s is surrounding field structure parameter, Q is charge, w_s is equation of state parameter and M is mass of the black hole. By considering $\lambda = 0$ and $k = 8\pi G_N$, this metric regains the Reissner-Nordström black hole surrounded by a surrounding field as [42]

$$ds^2 = - \left(1 - \frac{2M}{r} + \frac{Q^2}{r^2} - \frac{N_s}{r^{3w_s+1}} \right) dt^2 + \frac{dr^2}{\left(1 - \frac{2M}{r} + \frac{Q^2}{r^2} - \frac{N_s}{r^{3w_s+1}} \right)} + r^2 d\Omega^2. \quad (2.4)$$

We use the metric (2.2) to investigate the thermodynamic geometry of a black hole surrounded by perfect fluid in Rastall theory. In particular, we consider the quintessence and dust fields as sub-classes of the Rastall fields.

3 Black hole surrounded by the quintessence field

In this section, we are going to investigate the thermodynamic properties of a black hole surrounded by the quintessence field. A quintessence field plays important role for the observed accelerated expansion of the universe [42]. By considering $w_s = w_q = -\frac{2}{3}$, the metric (2.2) takes the following form:

$$ds^2 = -f_q(r)dt^2 + \frac{dr^2}{f_q(r)} + r^2 d\Omega^2, \quad (3.1)$$

$$f_q(r) = 1 - \frac{2M}{r} + \frac{Q^2}{r^2} - \frac{N_q}{r^{\frac{-1-2k\lambda}{1-k\lambda}}}. \quad (3.2)$$

For the case $k\lambda = \frac{1}{4}$, metric (3.1) can be written as

$$ds^2 = -f_q(r)dt^2 + \frac{dr^2}{f_q(r)} + r^2 d\Omega^2, \quad (3.3)$$

$$f_q(r) = 1 - \frac{2M}{r} + \frac{Q^2}{r^2} - N_q r^2. \quad (3.4)$$

3.1 Thermodynamics

The mass corresponding to Eq. (3.3), can be obtain using $f_q(r) = 0$. Also, we can express the mass of the black hole M , in terms of its entropy S , using the relation between entropy S and event horizon radius r_+ ($S = \pi r_+^2$), as

$$M(S, N_q, Q) = \frac{\pi^2 Q^2 + \pi S - N_q S^2}{2\pi^{\frac{3}{2}} S^{\frac{1}{2}}}. \quad (3.5)$$

First law of thermodynamics for a black hole surrounded by quintessence field can be written as

$$dM = TdS + \Psi dN_q + \varphi dQ, \quad (3.6)$$

where φ is a quantity conjugate to electric charge Q and Ψ is a quantity conjugate to quintessence parameter N_q . So, by using the Eqs. (3.5) and (3.6), we obtain thermodynamic parameters like temperature ($T = \frac{\partial M}{\partial S}$), heat capacity ($C = T \frac{\partial S}{\partial T}$), ($\Psi = \frac{\partial M}{\partial N_q}$), and ($\varphi = \frac{\partial M}{\partial Q}$) as follows

$$T = -\frac{\pi^2 Q^2 - \pi S + 3N_q S^2}{4\pi^{\frac{3}{2}} S^{\frac{3}{2}}}, \quad (3.7)$$

$$C = -\frac{2S(\pi^2 Q^2 - \pi S + 3N_q S^2)}{3\pi^2 Q^2 - \pi S - 3N_q S^2}, \quad (3.8)$$

$$\varphi = \sqrt{\frac{\pi}{S}} Q, \quad (3.9)$$

$$\Psi = -\frac{1}{2} \left(\frac{S}{\pi} \right)^{3/2}. \quad (3.10)$$

These thermodynamic parameters are plotted in terms of horizon radius r_+ , (see Fig. 1).

From Fig. 1(a), we find that for $N_q = 0.05$, the mass of this black hole has a minimum value at $r_1 = 0.51$, afterword it arrives to its maximum value at $r_2 = 2.53$, then it becomes zero at $r_0 = 4.5$. Also, the behaviour of the temperature versus r_+ is demonstrated in Fig. 1(b). From this figure, we see that for low values of r_+ , the temperature increases to a maximum point and then it starts decreasing with higher r_+ . In other words, temperature is positive only in a particular range of event horizon ($r_1 < r_+ < r_2$) for $N_q = 0.05$, however, at $r < r_1$, and $r_2 < r$, it will be negative and leads to an unphysical solution. In addition, Fig. 1(c) show that the increase in the values of quintessence factor (N_q) decrease the temperature of black hole surrounded by quintessence. In other words, increasing in the values of quintessence the physical area of this black hole decreases. Moreover, in Fig. 1(d), the behaviour of the heat capacity versus r_+ is represented. Note that, the roots of heat capacity represent a physical limitation points and the divergences of the heat capacity demonstrate phase transition critical points of black hole [41]. From Fig. 1(d), we see that the heat capacity of this black hole will be zero at r_1 and r_2 , which means that it has two physical limitation points. Furthermore, it diverges at $r_+ = r_\infty = 0.825$ and thus it has one phase transition critical point. This results that the heat capacity is negative at $r_+ < r_1$, which means that the black hole system is unstable. Then, at $r_1 < r_+ < r_\infty$, the heat capacity is positive, which means that it is in stable phase. Next, at $r_\infty < r_+ < r_2$, it crashes in to a negative region (unstable phase) and, at $r_+ > r_2$, it becomes stable. Further, for the case $N_q = 0$, the physical limitation points get changed, and there will be only one physical limitation points. Moreover, the behaviour of φ as a quantity conjugate to electric charge Q and Ψ as a quantity conjugate to quintessence parameter N_q versus r_+ are shown in Fig. 1(e), (f). As can be seen, φ has a maximum value at $r_+ = 0.333$, afterword it starts decreasing with higher r_+ , and Ψ starts from zero and then it falls into a negative region.

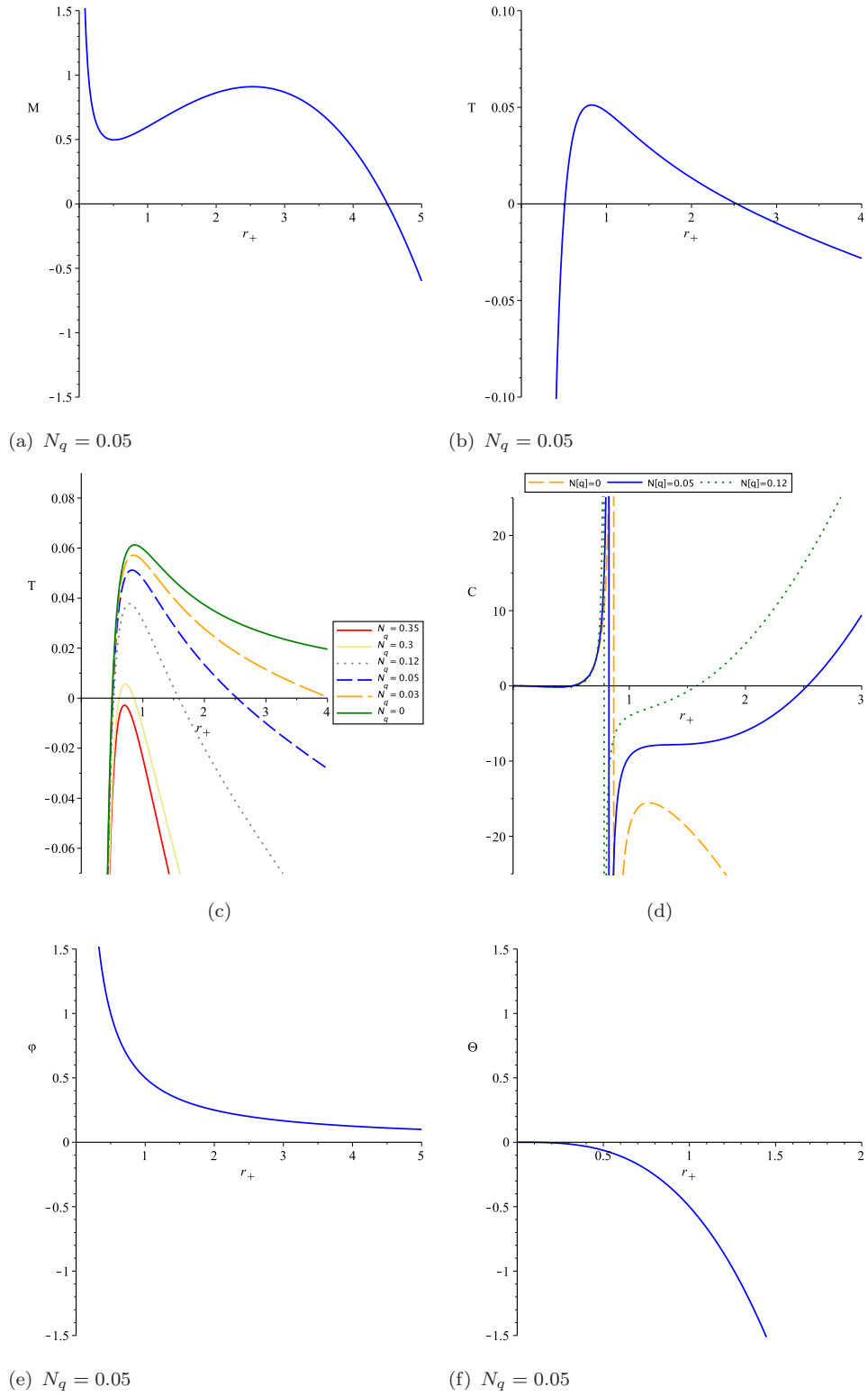


Figure 1: Variations of thermodynamic parameters of a black hole surrounded by quintessence field in terms of horizon radius r_+ for $Q = \sqrt{0.25}$.

3.2 Thermodynamic geometry

In this section, based on geometric formalism suggested by Weinhold, Ruppiner, Quevedo and HPEM, we create the geometric structure for a black hole surrounded by quintessence. The Weinhold geometry is specified in mass representation as [35]

$$g_{ij}^W = \partial_i \partial_j M(S, N_q, Q). \quad (3.11)$$

In this case, the line element for a black hole surrounded by quintessence is

$$\begin{aligned} ds_W^2 = & M_{SS} dS^2 + M_{N_q N_q} dN_q^2 + M_{QQ} dQ^2 + 2M_{SN_q} dS dN_q \\ & + 2M_{SQ} dS dQ + 2M_{N_q Q} dN_q dQ, \end{aligned} \quad (3.12)$$

so the matrix

$$g^W = \begin{bmatrix} M_{SS} & M_{SN_q} & M_{SQ} \\ M_{N_q S} & 0 & 0 \\ M_{QS} & 0 & M_{QQ} \end{bmatrix}. \quad (3.13)$$

We use the above equations to obtain the curvature scalar of the Weinhold metric (R^W)

$$R^W = 0. \quad (3.14)$$

The curvature scalar in the Weinhold formalism is equal to zero, thus we cannot describe the phase transition of this thermodynamic system. Next, we consider the Ruppiner geometry. Through the conformal property, the Ruppiner metric in the thermodynamic system is defined as [34, 43, 44]

$$ds_R^2 = \frac{1}{T} ds_W^2, \quad (3.15)$$

and the relevant matrix is

$$g^R = \left(\frac{4\pi^{\frac{3}{2}} S^{\frac{3}{2}}}{S\pi - \pi^2 Q^2 - 3S^2 N_q} \right) \begin{bmatrix} M_{SS} & M_{SN_q} & M_{SQ} \\ M_{N_q S} & 0 & 0 \\ M_{QS} & 0 & M_{QQ} \end{bmatrix}. \quad (3.16)$$

Therefore, the curvature scalar of the Ruppiner geometry is given by

$$R^{Rup} = -1/4 \frac{\sqrt{S} (17\pi^2 Q^2 - 9S^2 N_q - 7\pi S)}{(\pi^2 Q^2 + 3S^2 N_q - \pi S) \pi^{3/2}} \left(\frac{S}{\pi} \right)^{-3/2}. \quad (3.17)$$

The resulting curvature scalar is plotted versus horizon radius to investigate thermodynamic phase transition (see Fig. 2). It can be observed from this figure that the singular points of the curvature scalar of Ruppeiner metric coincide with zero points of the heat capacity. Moreover, variations of Ruppeiner metric and the heat capacity in terms of different values of quintessence factor (N_q), are shown in Figs. 2(b) and 1(d). As one can see from these Figures, the change in the values of quintessence factor causes the change in zero points of the heat capacity and also, singular points of the curvature scalar of Ruppeiner metric. But in any case, for both low

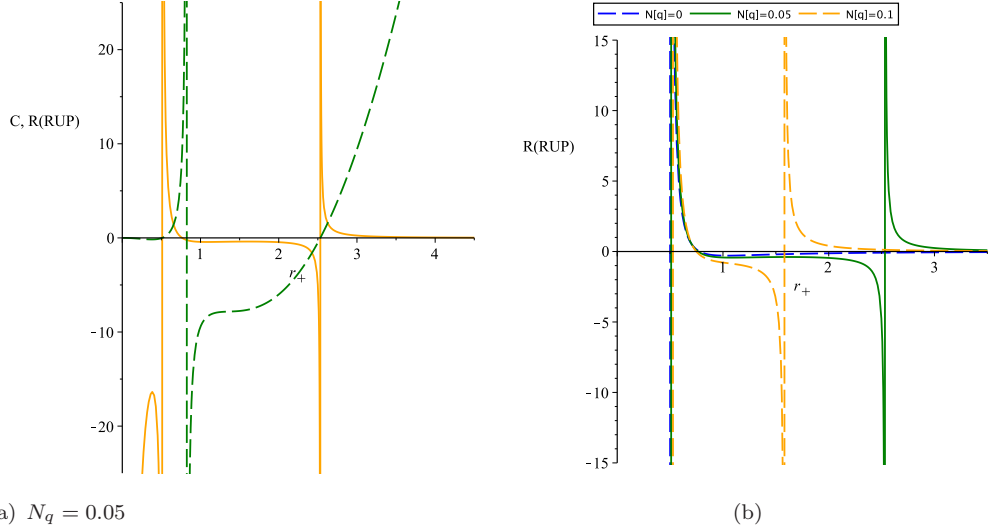


Figure 2: (a) Curvature scalar variation of Ruppeiner metric (orange line) and the heat capacity (green dash line) of a black hole surrounded by quintessence field and (b) Curvature scalar variation of Ruppeiner metric for different values of quintessence factor, in terms of horizon radius r_+ for $Q = \sqrt{0.25}$.

and high value of the quintessence factor, again the singular points of the curvature scalar of Ruppeiner metric entirely coincide with zero points of the heat capacity.

Now, we will use the Quevedo and HPEM formalism to discuss the thermodynamic properties of the black hole. The general form of the metric in Quevedo formalism is given as [38, 45]:

$$g = \left(E^c \frac{\partial \Phi}{\partial E^c} \right) \left(\eta_{ab} \delta^{bc} \frac{\partial^2 \Phi}{\partial E^c \partial E^d} dE^a dE^d \right), \quad (3.18)$$

in which

$$\frac{\partial \Phi}{\partial E^c} = \delta_{cb} I^b, \quad (3.19)$$

where E^a and I^b are the extensive and intensive thermodynamic variables, respectively, and Φ is the thermodynamic potential. Also, the generalized HPEM metric with n extensive variables ($n \geq 2$) has the following form [39–41]

$$ds_{HPEM}^2 = \frac{SM_S}{\left(\prod_{i=2}^n \frac{\partial^2 M}{\partial \chi_i^2} \right)^3} \left(-M_{SS} dS^2 + \sum_{i=2}^n \left(\frac{\partial^2 M}{\partial \chi_i^2} \right) d\chi_i^2 \right), \quad (3.20)$$

In which, $\chi_i (\chi_i \neq S)$, $M_S = \frac{\partial M}{\partial S}$ and $M_{SS} = \frac{\partial^2 M}{\partial S^2}$ are extensive parameters. Moreover, The Quevedo and HPEM metrics can be written as [39–41]

$$ds^2 = \begin{cases} (SM_S + N_q M_{N_q} + Q M_Q) (-M_{SS} dS^2 + M_{N_q N_q} dN_q^2 + M_{Q Q} dQ^2) & \text{Quevedo Case I} \\ SM_S (-M_{SS} dS^2 + M_{N_q N_q} dN_q^2 + M_{Q Q} dQ^2) & \text{Quevedo Case II} \\ \frac{SM_S}{\left(\frac{\partial^2 M}{\partial N_q^2} \frac{\partial^2 M}{\partial Q^2} \right)^3} (-M_{SS} dS^2 + M_{N_q N_q} dN_q^2 + M_{Q Q} dQ^2) & \text{HPEM} \end{cases} \quad (3.21)$$

These metrics have following denominator for their Ricci scalars [40, 41]

$$\text{denom}(R) = \begin{cases} 2M_{SS}^2 M_{N_q N_q}^2 M_{QQ}^2 (SM_S + N_q M_{N_q} + QM_Q)^3 & \text{Quevedo Case I} \\ 2S^3 M_{SS}^2 M_{N_q N_q}^2 M_{QQ}^2 M_S^3 & \text{Quevedo Case II} \\ 2S^3 M_{SS}^2 M_S^3 & \text{HPEM} \end{cases} \quad (3.22)$$

Solving the mentioned equations, It is evident that in case of Quevedo formalism, we can't find any physical data about the system. But, in case of HPEM metric, as shown in Fig. 3, divergencies of the Ricci scalar and zero points of the heat capacity will coincide. Of course, there is another divergency of HPEM metric which coincides with the singular points of heat capacity. Actually the denominator of the Ricci scalar of HPEM metric only contains numerator and denominator of the heat capacity. In other words, divergence points of the Ricci scalar of HPEM metric coincide with both types of phase transitions of the heat capacity. Therefore, It seems we can extract more information of HPEM metric compared with Ruppeiner metric.

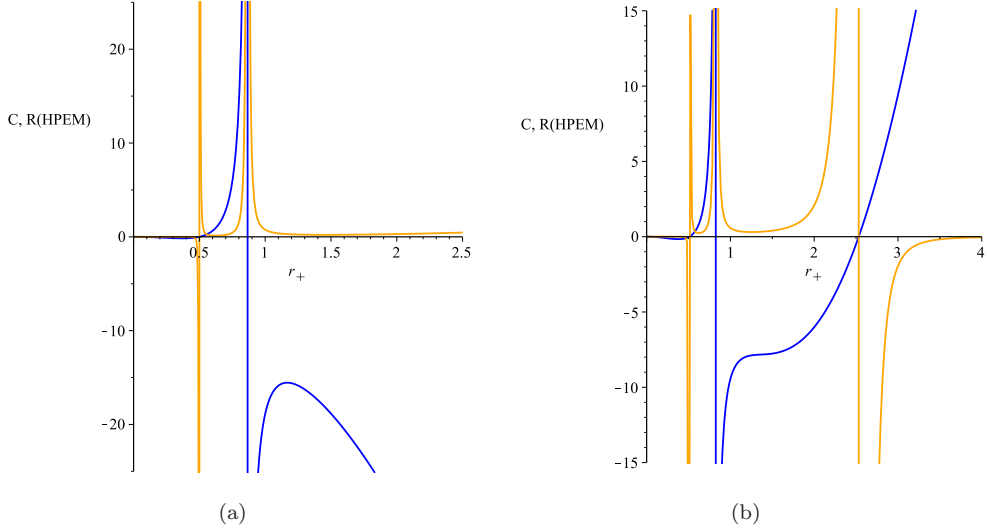


Figure 3: Curvature scalar variation of HPEM metric (orange line) and heat capacity (blue line) of a black hole surrounded by quintessence field in terms of horizon radius r_+ for $Q = \sqrt{0.25}$ and $N_q = 0$, $N_q = 0.05$ for (a) and (b) respectively.

4 Black hole surrounded by dust field

In this section, we consider a black hole surrounded by the dust field. So, by putting $w_s = w_d = 0$ and $k\lambda = \frac{2}{9}$, the Eq. (2.2) can be written as [12]

$$ds^2 = -f_d(r)dt^2 + \frac{dr^2}{f_d(r)} + r^2 d\Omega^2, \quad (4.1)$$

$$f_d(r) = 1 - \frac{2M}{r} + \frac{Q^2}{r^2} - N_d r. \quad (4.2)$$

4.1 Thermodynamics

In this section, we investigate thermodynamical behaviour of a black hole surrounded by dust field. In this case, mass of the black hole M , in terms of its entropy S , can be written as

$$M(S, N_d, Q) = \frac{\pi^2 Q^2 + \pi S - N_d S^{\frac{3}{2}} \pi^{\frac{1}{2}}}{2\pi^{\frac{3}{2}} S^{\frac{1}{2}}}, \quad (4.3)$$

and the first law of thermodynamics for this black hole is

$$dM = TdS + \Psi dN_q + \varphi dQ, \quad (4.4)$$

So, by using the above equations (4.3, 4.4), the thermodynamic parameters can be obtained as

$$T = -\frac{\pi^2 Q^2 - \pi S + 2N_d S^{\frac{3}{2}} \pi^{\frac{1}{2}}}{4\pi^{\frac{3}{2}} S^{\frac{3}{2}}}, \quad (4.5)$$

$$C = -\frac{2S \left(\pi^2 Q^2 - \pi S + 2N_d S^{\frac{3}{2}} \pi^{\frac{1}{2}} \right)}{3\pi^2 Q^2 - \pi S}, \quad (4.6)$$

$$\varphi = \sqrt{\frac{\pi}{S}} Q, \quad (4.7)$$

$$\Psi = -\frac{1}{2} \frac{S}{\pi}. \quad (4.8)$$

Plots of these thermodynamic parameters in terms of horizon radius r_+ , are shown in Figs. 4.

Fig. 4(a) shows that mass of this black hole has one minimum point at $r_1 = 0.513$. Also, it can be seen from Fig. 4(b) that temperature of this system is in the positive region at a particular range of event horizon radius r_+ . Moreover, similar to quintessence case, the increase in the values of dust factor (N_d) causes decrease in the temperature of a black hole surrounded by dust field. In addition, Fig. 4(c) shows that the heat capacity is in the negative region (unstable phase), afterword at r_1 , it becomes zero and Then for $r_+ > r_1$, it locate in positive region (stable phase). Moreover, it can be observed from Fig. 4(c) that for the case $N_q \neq 0$, there are two physical limitation points, and for the case $N_q = 0$, there will be only one physical limitation point. Furthermore, in Fig. 4(d), (e) variation of φ and Ψ versus r_+ are demonstrated. As can be seen, similar to quintessence case, φ has a maximum value at $r_+ = 0.333$, afterword it starts decreasing with higher r_+ , and Ψ starts from zero and then it falls into a negative region.

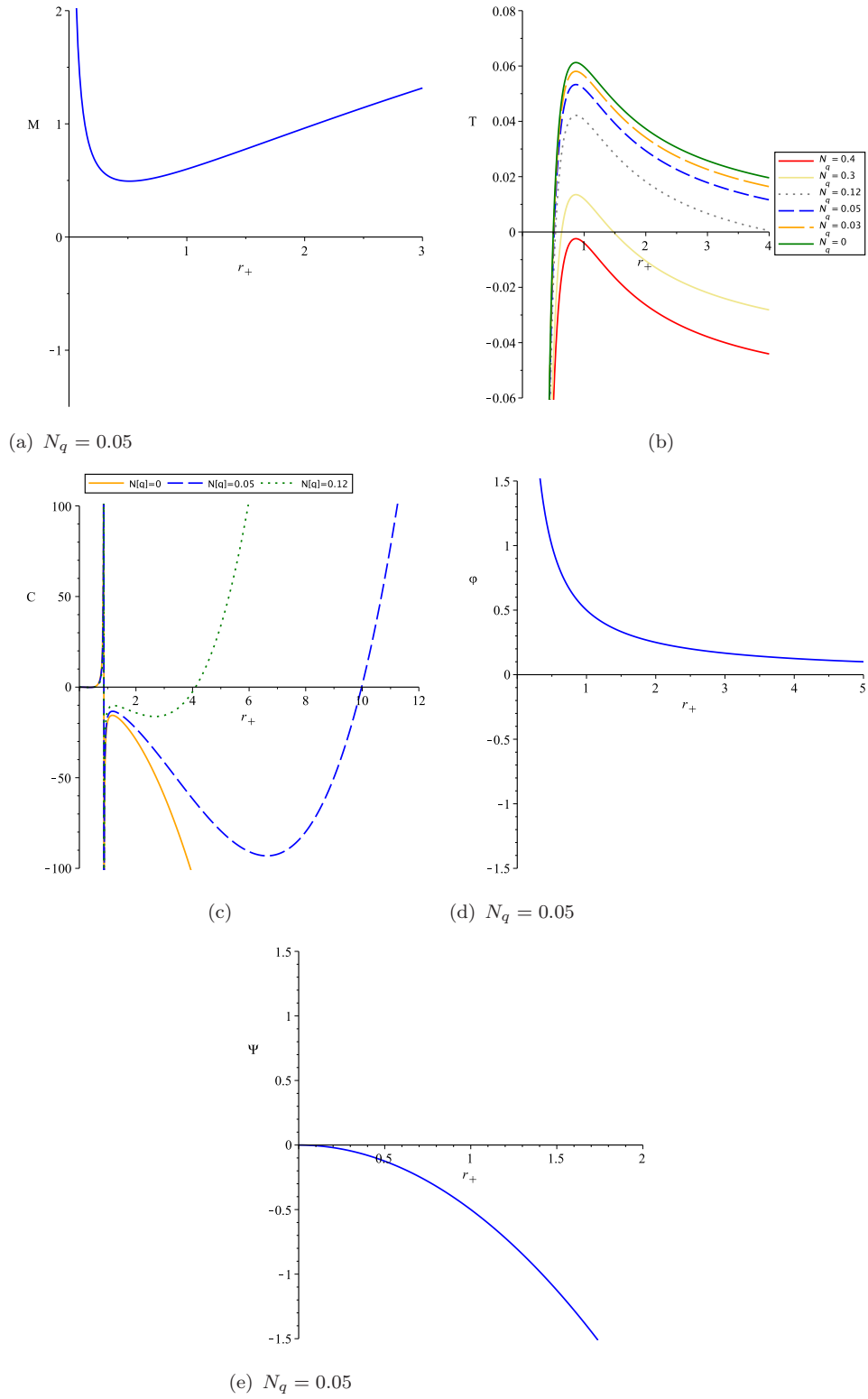


Figure 4: Variations of thermodynamic parameters of a black hole surrounded by dust field in terms of horizon radius r_+ for $Q = \sqrt{0.25}$.

4.2 Thermodynamic geometry

In this section, again we use the geometric formalism of Weinhold, Ruppiner, Quevedo and HPEM metrics of the thermal system, and investigate the physical limitation points and phase transition critical points of a black hole surrounded by dust field. we can use the following Weinhold metric [35]:

$$g_{ij}^W = \partial_i \partial_j M(S, N_d, Q), \quad (4.9)$$

and write the line element corresponding to Weinhold metric for this system in mass representation as

$$ds_W^2 = M_{SS} dS^2 + M_{N_d N_d} dN_d^2 + M_{QQ} dQ^2 + 2M_{SN_d} dS dN_d + 2M_{SQ} dS dQ + 2M_{N_d Q} dN_d dQ. \quad (4.10)$$

Therefore, the relevant matrix is

$$g^W = \begin{bmatrix} M_{SS} & M_{SN_d} & M_{SQ} \\ M_{N_d S} & 0 & 0 \\ M_{QS} & 0 & M_{QQ} \end{bmatrix}, \quad (4.11)$$

and the curvature scalar of the Weinhold metric for this system is

$$R^W = 0. \quad (4.12)$$

So, the Weinhold formalism suggests that black hole surrounded by dust field is flat and we cannot investigate the phase transition of this thermodynamic system. Moreover, we consider Ruppiner formalism in which line element is conformally transformed to the Weinhold metric as [34, 43, 44]

$$ds_R^2 = \frac{1}{T} ds_W^2. \quad (4.13)$$

The matrix corresponding to this metric is

$$g^R = \left(\frac{4\pi^{\frac{3}{2}} S^{\frac{3}{2}}}{S\pi - \pi^2 Q^2 - 2S^{\frac{3}{2}} N_d \pi^{\frac{3}{2}}} \right) \begin{bmatrix} M_{SS} & M_{SN_d} & M_{SQ} \\ M_{N_d S} & 0 & 0 \\ M_{QS} & 0 & M_{QQ} \end{bmatrix}, \quad (4.14)$$

and the relevant scalar curvature is

$$R^{Rup} = 1/4 \frac{4 N_d S^{3/2} \sqrt{\pi} - 13 \pi^2 Q^2 + 3 \pi S}{(2 N_d S^{3/2} \sqrt{\pi} + \pi^2 Q^2 - \pi S) S}. \quad (4.15)$$

Plot of this scalar curvature is demonstrated in Fig. 5(a). Moreover, plot of the curvature scalar variation of the Ruppiner metric and heat capacity, in terms of r_+ is shown in Fig. 5(b). It can be seen from Fig. 5(a), (b) that changes in the value of dust factor cause change in the singular points of the curvature scalar of Ruppeiner metric and also in zero points of heat capacity. Moreover, similar to quintessence case, for both low and high values of dust factor, the singular points of the curvature scalar of Ruppeiner metric entirely coincides with zero points of heat capacity.

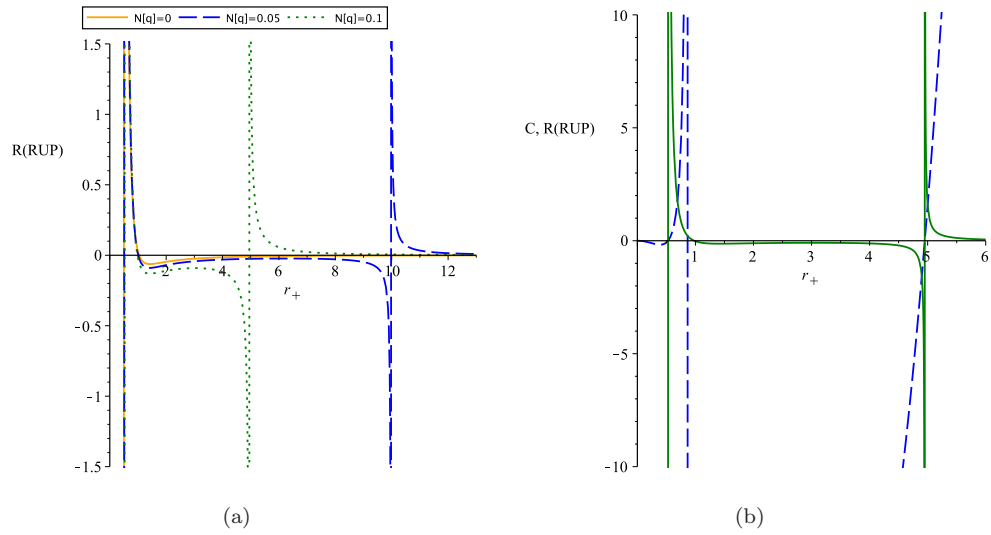


Figure 5: (a) Curvature scalar variation of Ruppeiner metric for different values of dust factor, and (b) Curvature scalar variation of Ruppeiner metric (green continuous line) and heat capacity (blue dash line) of a black hole surrounded by dust field in terms of horizon radius r_+ for $N_d = 0.1$, $Q = \sqrt{0.25}$.

Now, to extend the analysis, we consider the Quevedo and HPEM metrics as [39–41]

$$ds^2 = \begin{cases} (SM_S + N_d M_{N_d} + Q M_Q)(-M_{SS} dS^2 + M_{N_d N_d} dN_d^2 + M_{QQ} dQ^2) & \text{Quevedo Case I} \\ SM_S(-M_{SS} dS^2 + M_{N_d N_d} dN_d^2 + M_{QQ} dQ^2) & \text{Quevedo Case II} \\ \frac{SM_S}{\left(\frac{\partial^2 M}{\partial N_d^2} \frac{\partial^2 M}{\partial Q^2}\right)^3} (-M_{SS} dS^2 + M_{N_d N_d} dN_d^2 + M_{QQ} dQ^2) & \text{HPEM} \end{cases} \quad (4.16)$$

These metrics have following denominator for their Ricci scalars [40, 41]

$$\text{denom}(R) = \begin{cases} 2M_{SS}^2 M_{N_d N_d}^2 M_{QQ}^2 (SM_S + N_d M_{N_d} + Q M_Q)^3 & \text{Quevedo Case I} \\ 2S^3 M_{SS}^2 M_{N_d N_d}^2 M_{QQ}^2 M_S^3 & \text{Quevedo Case II} \\ 2S^3 M_{SS}^2 M_S^3 & \text{HPEM} \end{cases} \quad (4.17)$$

Solving the above equations, again similar to the quintessence section for the case of Quevedo formalism, we can't find any physical data about the system. However, in case of HPEM metric, as shown in Fig. 6, divergencies of the Ricci scalar coincide with zero points of the heat capacity. But, In comparison with Ruppeiner metric, we can see another divergency of HPEM metric which coincides with the singular points of heat capacity. So, divergence points of the Ricci scalar of HPEM metric coincide with both types of phase transitions of the heat capacity.

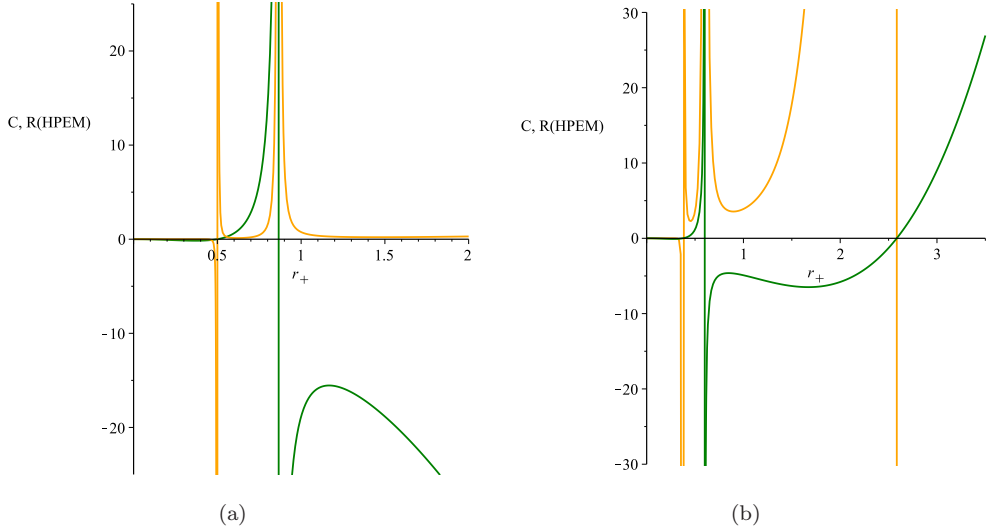


Figure 6: Curvature scalar variation of HPEM metric (orange line) and heat capacity (green line) of a black hole surrounded by dust field in terms of horizon radius r_+ for $Q = \sqrt{0.25}$, $N_q = 0$ and $Q = \sqrt{0.12}$, $N_q = 0.19$ for (a) and (b) respectively.

5 Concluding remarks

One possible explanation to the negative pressure in an expanding universe is that the universe is filled with a peculiar kind of perfect fluid, where the proportion between the pressure and energy

density is between 1 and $1/3$. If this is so, then it becomes important to study the interaction of the strong gravity objects such as black holes with such fluid. This idea is proposed by Kiselev [42], and has further been generalized to the Rastall model of gravity [12].

In this paper, we have considered a black hole surrounded by a generic perfect fluid in Rastall theory to emphasize its thermodynamics. To make the analysis clear, we have focused on two special cases of the perfect fluid. First, we have derived an expression for the mass of black hole surrounded by quintessence field. The resulting mass of this system has a minimum value for small horizon radius r_+ , afterword it arrives to its maximum value for a bit higher value of r_+ , then vanishes for larger r_+ . By exploiting standard thermodynamic relations, we have derived the Hawking temperature and heat capacity. It is known that negative heat capacity corresponds to instability, however the positive value of heat capacity describe stable black holes. In order to study the behavior of thermodynamic entities obtained for black hole surrounded by both quintessence field and dust field, we have plotted the graphs with respect to event horizon. For the figure, it is clear that temperature of black hole surrounded by quintessence field in Rastall theory remains positive only for the specific values of event horizon for quintessence factor $N_q = 0.05$. It is also found that the increasing in the values of quintessence the physical area of this black hole decrease. For heat capacity plot, we have found that there exist two physical limitation points for the system at two different values of event horizons. Here we note that the stability do not occur corresponding to all horizon radius. Further, we have studied the geometric structure of the black hole surrounded by quintessence field. This is done by calculating the Weinhold, Ruppiner, Quevedo and HPEM curvature scalars. We find that Weinhold curvature scalar vanishes and in this situation one can not describe the phase transition. As well as, we have derived the curvature scalar of Quevedo metric and haven't found any physical data about the system. The curvature scalar for the Ruppiner and the HPEM geometry does not vanishes. The curvature scalar for the Ruppiner and the HPEM geometry suggests that the singular points coincide with zero points of the heat capacity. Also, we have observed another divergency of HPEM metric which coincides with the singular points of heat capacity. So, divergence points of the Ricci scalar of HPEM metric coincide with both types of phase transitions of the heat capacity. Therefore, It can be extracted more information from HPEM metric compared with other mentioned metrics.

Moreover, the thermodynamic properties of black hole surrounded by dust field in Rastall gravity are also studied. Following the earlier case, we have calculated the mass, Hawking temperature and heat capacity here also. To emphasize the behavior of these quantities, we have plotted the graphs with respect to event horizon. From the figure, we have found that the mass of the system has one minimum point at particular value of horizon radius. The behavior of temperature with horizon radius is similar to the quintessence case, i.e., increasing in the values of quintessence the physical area of this black hole decrease. From the plot, we have seen that stability of black hole increases with the size of black hole upto a certain point. After that point a phase transition occurs and converts the black hole in to the more unstable state. The geometric properties of black hole is studied in this case also. It would be interesting to discuss the effect of thermal fluctuations on thermodynamics of the black hole surrounded by Rastall

gravity.

References

- [1] P. Rastall, *Phys. Rev. D* **6**, 3357 (1972).
- [2] T. Josset, A. Perez, *Phys. Rev. Lett.* **118**, 021102 (2017).
- [3] J. P. Campos, J. C. Fabris, R. Perez, O. F. Piattella, H. Velten, *Eur. Phys. J. C* **73**, 2357 (2013).
- [4] J. C. Fabris, M. H. Daouda, O. F. Piattella, *Phys. Lett. B* **711**, 232 (2012).
- [5] H. Moradpour, *Phys. Lett. B* **757**, 187 (2016).
- [6] C. E. M. Batista, M. H. Daouda, J. C. Fabris, O. F. Piattella, D. C. Rodrigues, *Phys. Rev. D* **85**, 084008 (2012).
- [7] C. Wolf, *Phys. Scr.* **34**, 193 (1986).
- [8] H. Moradpour, Y. Heydarzade, F. Darabi, I. G. Salako, *Eur. Phys. J. C* **77**, 259 (2017).
- [9] A. M. Oliveira, H. E. S. Velten, J. C. Fabris, L. Casarini, *Phys. Rev. D* **92**, 044020 (2015).
- [10] A. M. Oliveira, H. E. S. Velten, J. C. Fabris, *Phys. Rev. D* **93**, 124020 (2016).
- [11] K. A. Bronnikov, J. C. Fabris, O. F. Piattella, E. C. Santos, *Gen. Relativ. Gravit.* **48**, 162 (2016).
- [12] Y. Heydarzade, F. Darabi, *Phys. Lett. B* **771**, 365 (2017).
- [13] M. S. Ma, R. Zhao, *Eur. Phys. J. C* **77**, 629 (2017).
- [14] S. Soroushfar and M. Afrooz, arXiv:1806.00620 [gr-qc].
- [15] S. W. Hawking, *Nature* **248**, 30 (1974).
- [16] J. D. Bekenstein, *Phys. Rev. D* **7**, 2333 (1973).
- [17] S. W. Hawking, D. N. Page, *Commun. Math. Phys.* **87**, 577 (1983).
- [18] J. Maldacena, *Adv. Theor. Math. Phys.* **2**, 231 (1998).
- [19] E. Witten, *Adv. Theor. Math. Phys.* **2**, 505 (1998).
- [20] A. Sahay, T. Sarkar, G. Sengupta, *JHEP*, 2010, 125 (2010).
- [21] Q. J. Cao, Y. X. Chen, K. N. Shao, *Phys. Rev. D* **83**, 064015 (2011).
- [22] D. Kubiznak, R. B. Mann, *JEHP*, 2012, 33 (2012).
- [23] S. Soroushfar, R. Saffari and N. Kamvar, *Eur. Phys. J. C* **76**, no. 9, 476 (2016) doi:10.1140/epjc/s10052-016-4311-6 [arXiv:1605.00767 [gr-qc]].
- [24] K. K. J. Rodrigue, M. Saleh, B. B. Thomas and T. C. Kofane, arXiv:1808.03474 [gr-qc].
- [25] S. Upadhyay, B. Pourhassan, *Prog. Theor. Exp. Phys.* 013B03 (2019).
- [26] S. Upadhyay, S. Soroushfar and R. Saffari, arXiv:1801.09574 [gr-qc].
- [27] S. Upadhyay, *Gen. Rel. Grav.* **50**, 128 (2018).
- [28] S. Upadhyay, S. H. Hendi, S. Panahiyan, B. E. Panah, *Prog. Theor. Exp. Phys.* 093E01 (2018).
- [29] S. H. Hendi, S. Panahiyan, S. Upadhyay, B. E. Panah, *Phys. Rev. D* **95**, 084036 (2017).
- [30] S. Upadhyay, *Phys. Lett. B* **775**, 130 (2017).

- [31] S. Upadhyay, B. Pourhassan, H. Farahani, Phys. Rev. D. 95, 106014 (2017).
- [32] B. Pourhassan, S. Upadhyay, H. Saadat, H. Farahani, Nucl. Phys. B 928, 415 (2018)..
- [33] B. Pourhassan, S. Upadhyay, H. Farahani, arXiv:1701.08650 [physics.gen-ph].
- [34] G. Ruppeiner, Phys. Rev. A 20, 1608 (1979).
- [35] F. Weinhold, J. Chem. Phys 63, 2479 (1975).
- [36] P. Salamon, E. Ihrig, R. S. Berry, J. Math. Phys. 24, 2515 (1983).
- [37] R. Mrugala, J. D. Nulton, J. C. Schon, P. Salamon, Phys. Rev. A 41, 3156 (1990).
- [38] H. Quevedo, J. Math. Phys. 48 (2007) 013506.
- [39] S. H. Hendi, S. Panahiyan, B. Eslam Panah and M. Momennia, Eur. Phys. J. C **75**, no. 10, 507 (2015) doi:10.1140/epjc/s10052-015-3701-5 [arXiv:1506.08092 [gr-qc]].
- [40] S. H. Hendi, A. Sheykhi, S. Panahiyan and B. Eslam Panah, Phys. Rev. D **92**, no. 6, 064028 (2015) doi:10.1103/PhysRevD.92.064028 [arXiv:1509.08593 [hep-th]].
- [41] B. Eslam Panah, Phys. Lett. B **787**, 45 (2018) doi:10.1016/j.physletb.2018.10.042 [arXiv:1805.03014 [hep-th]].
- [42] V. V. Kiselev, Class. Quantum. Grav 20, 1187 (2003).
- [43] P. Salamon, J. D. Nulton and E. Ihrig, J. Chem. Phys, 80,436 (1984).
- [44] R. Mrugala, Physica. A (Amsterdam), 125, 631 (1984).
- [45] H. Quevedo, J. Math. Phys. **48** (2007) 013506 [physics/0604164].